Low sticking probability in the nonactivated dissociation of N_2 molecules on W(110)

M. Alducin[a)]
Donostia International Physics Center (DIPC), P. Manuel de Lardizabal 4, 20018 San Sebastián, Spain

R. Díez Muiño
Donostia International Physics Center (DIPC), P. Manuel de Lardizabal 4, 20018 San Sebastián, Spain and Unidad de Física de Materiales, Centro Mixto CSIC-UPV/EHU, Facultad de Químicas, UPV/EHU, Apartado 1072, 20080 San Sebastián, Spain

H. F. Busnengo
Donostia International Physics Center (DIPC), P. Manuel de Lardizabal 4, 20018 San Sebastián, Spain; Instituto de Física Rosario (CONICET-UNR) and Facultad de Ciencias Exactas, Ingeniería y Agrimensura, Universidad Nacional de Rosario, Avenida Pellegrini 250, 2000 Rosario, Argentina

A. Salin
Donostia International Physics Center (DIPC), P. Manuel de Lardizabal 4, 20018 San Sebastián, Spain

(Received 12 July 2006; accepted 22 August 2006; published online 10 October 2006)

The six-dimensional potential energy surface for the dissociation of N_2 molecules on the W(110) surface has been determined by density functional calculations and interpolated using the corrugation reducing procedure. Examination of the resulting six-dimensional potential energy surface shows that nonactivated paths are available for dissociation. In spite of this, the dissociation probability goes to a very small value when the impact energy goes to zero and increases with increasing energy, a behavior usually associated with activated systems. Statistics on the dynamics indicate that this unconventional result is a consequence of the characteristics of the potential energy surface at long distances. Furthermore, two distinct channels are identified in the dissociation process, namely, a direct one and an indirect one. The former is responsible for dissociation at high energies. The latter, which includes long-lasting dynamic trapping in the vicinity of a potential well above the W top position, is the leading mechanism at low and intermediate energies. © *2006 American Institute of Physics*. [DOI: 10.1063/1.2355672]

I. INTRODUCTION

The interaction of N_2 molecules with metal surfaces has been thoroughly studied over the last decades. Dissociation of N_2 is, for instance, the rate-limiting step in ammonia synthesis, one of the most important catalyzed reactions in the chemical industry. Particularly intriguing is the dissociation of N_2 on tungsten surfaces. Early studies based on work function measurements and flash desorption spectroscopy showed that N_2 on W has the largest crystallographic anisotropies as regards adsorption yields and sticking coefficients.[1,2] The most dramatic example of this anisotropy is the value of the zero-coverage sticking probability that varies from ≈ 0.59 on W(100) to $\approx 5\times 10^{-3}$ on W(110) at room temperature. The system has therefore been considered as emblematic to understand the influence of surface structure in chemisorption. This has motivated a wealth of experimental studies, mostly based on thermal desorption measurements, aimed at characterizing the adsorption of nitrogen on tungsten. Three different adsorption states are found:[2] the molecular α-N_2 state which desorbs near 300 K and is preferably formed on W(111) but not on W(110) or W(100); the weakly bound γ-N_2, a different molecular state observed on the various W faces, which desorbs near 150 K; and the strongly bound atomic β-N state that desorbs near 1000 K and exhibits similar adsorption energies on W(110) and W(100). Precisely, this similarity was considered a striking result in view of the different sticking coefficients observed in these two surfaces.

The low dissociation rate on the (110) face was initially attributed either to surface defects or to dissociation on stepped vicinal regions followed by surface diffusion.[3] Further studies finally confirmed that the dissociative chemisorption of N_2 takes place slowly but steadily on perfect W(110) even at low energies.[4] However, the actual mechanism for this process is still under discussion. Nitrogen on W(110) represents an interesting case, in which both weak molecular and dissociative chemisorption can occur, depending on the surface temperature T_s. For $T_s \leqslant 100$ K, N_2 adsorption is entirely molecular. As the surface is warmed up to typical molecular desorption temperatures (below 150 K), an appreciable conversion from molecular γ-N_2 to atomic β-N is also observed.[4,5] The latter result has been interpreted as an indication that the barrier to dissociation from the γ-N_2 state has a height close to the molecular desorption energy. Nonetheless and despite the amount of experimental data, the reason for the low sticking probability is still unclear.

Advances in the use of thermal molecular beams allowed

a)Electronic mail: wapalocm@sq.ehu.es

to explore the dissociative adsorption dynamics of N_2 on the W(110) surface from a different perspective.[6,7] Experiments were carried out at $T_s = 800$ K. At this surface temperature no molecular adsorption takes place. Measurements of the initial sticking coefficient S_0 as a function of the N_2 initial kinetic energy E_i show that S_0 is nearly constant ($\sim 10^{-3}$) for low E_i, then increases rather quickly in the range of $0.4 < E_i < 1.2$ eV and levels off at higher E_i.[6] This S-type curve, among other arguments, has led to conclude that the dissociation of N_2 on W(110) is an activated process.[4–8] Furthermore, the values of $S_0(E_i)$ obtained for different incidence angles exhibit total kinetic energy scaling. The latter seems to indicate a loss of memory of the initial conditions ("scrambling" of velocities) and is usually attributed to some kind of intermediate state in the dissociation process.[9,10] This argument, however, was argued not to be consistent with the nearly specular reflection peak of the reflected N_2 molecules also measured in these experiments.[6] Specular reflection is commonly attributed to direct processes in which no intermediate state is important. In summary, neither direct nor indirect dissociative mechanisms are unambiguously supported by the experimental $N_2/W(110)$ data.

One of the first theoretical attempts to understand the dissociative dynamics of N_2 on the W(110) surface was based on stochastic classical trajectory calculations performed with a parametrized six-dimensional (6D) potential energy surface (PES).[10] The various parameters of the 6D PES were fixed to reproduce experimental values such as the activation barrier, adsorption energies, and the experimental sticking coefficient measured at normal incidence. This model explained the experimental $S_0(E_i)$ in terms of a direct dissociation mechanism, in which a large activation barrier (≈ 1 eV) was required. The improvement of *ab initio* methods over the last few years has allowed to obtain detailed adiabatic PESs. Recent calculations based on density functional theory[11] (DFT) examine the dissociation in the $N_2/W(110)$ system for initial kinetic energies in the range of 0.4–1.2 eV. According to the authors the dissociation would be indirect, i.e., dominated by molecular trapping. The experimental S-curve would thus be explained by an activation barrier to reach the molecular state. Hence, the existing theoretical studies are nonconclusive as well.

In the present work, we study the dissociative dynamics of N_2 molecules on the W(110) surface for initial kinetic energies of the molecule that cover the whole experimental energy range. The purpose is to understand the still unclear nature of the mechanisms leading to dissociation in this system, as well as the causes for the low sticking probabilities measured in this surface at low energies. To do so, we first construct a 6D PES from the interpolation of a sufficiently large number of *ab initio* energies. Then, we perform statistical classical trajectory calculations to analyze in detail how the dissociative dynamics of the molecules depends on initial kinetic energy. Our results show the existence of nonactivated dissociative paths, that involve the dynamic trapping of the N_2 molecules in the vicinity of a potential well above the W top position. In spite of this, the dissociative probability resembles that of an activated system, i.e., is nearly zero at low incidence energies and increases with energy except for molecular incident energies of 200–400 meV. Concerning the direct or indirect nature of the dissociation process, we find that both mechanisms may occur depending on the incidence energy of the molecules. Thus, for energies above 400 meV, the dissociation process is rather direct because the molecules can overcome most of the potential slopes appearing in their approach to the surface without going through the well. On the contrary, dissociation for lower energies is mostly indirect due to the long-lasting dynamic trapping of the molecules around the well. Finally, we find that the low dissociative probabilities obtained at thermal energies are due to the characteristics of 6D PES at large distances that restrict the access to that well.

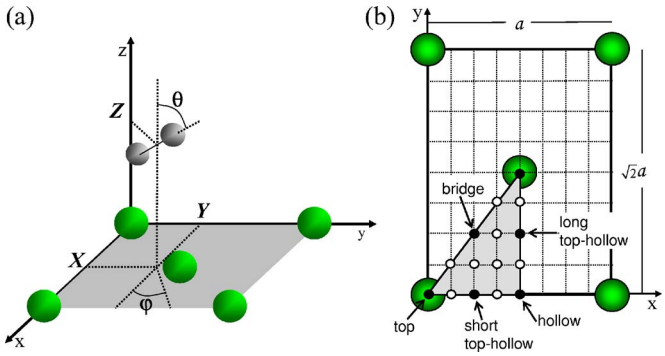

FIG. 1. (Color online) (a) Coordinate system used in our calculations: surface W atoms are in green and the N_2 nuclei are in gray. (b) Geometry of the W(110) surface. *Ab initio* calculations for N/W(110) have been performed for all sites marked by a circle. For $N_2/W(110)$, *ab initio* calculations have been performed for configurations for which the molecular center is over a site marked by a black circle. The shaded area shows the irreducible unit cell.

The outline of the paper is as follows. The details of *ab initio* calculations as well as the interpolation procedure used to construct the full 6D PES are described in Sec. II. The results obtained from classical trajectory calculations are shown and compared with available experimental data in Sec. III. Our main results and findings are summarized in Sec. IV.

II. CALCULATION OF THE POTENTIAL ENERGY SURFACE

The interaction energy of N_2 with the W(110) surface is described with a full adiabatic 6D PES that depends on the position of the molecular center defined as the center of nuclear charge of the molecule $\mathbf{R} \equiv (X, Y, Z)$, the molecular interatomic distance r and the molecular orientation relative to the surface determined by the polar and azimuthal angles (θ, φ). The coordinate system is depicted in Fig. 1(a). The 6D PES is constructed from the interpolation of 5610 *ab initio* energies using the *corrugation reducing procedure* (CRP).[12] The basic idea in this method is that the PES corrugation is mainly due to the interaction of each atom in the molecule with the surface atoms. In our case, the procedure consists in subtracting from the $N_2/W(110)$ interaction energy that of two isolated N atoms with the W(110) surface. To do so, the N/W(110) PES is also needed.

All *ab initio* data are obtained with DFT using the "Vienna *ab initio* simulation program"[13] (VASP) that operates

with a plane-wave basis set. The exchange-correlation energy is calculated with the generalized gradient approximation (GGA) and the Perdew-Wang energy functional (PW91). The electron-core interaction is described by ultrasoft pseudopotentials.[14] We have performed a series of preliminary calculations to determine the parameters that ensure that all *ab initio* energies are calculated to a prescribed accuracy. Thus, the energy cutoff in the plane-wave expansion is 348.1 eV. The fractional occupancies are determined through the broadening approach of Methfessel and Paxton[15] with $N=1$ and $\sigma=0.4$.

A. Slab determination

The theoretical lattice constant obtained from a bulk calculation is $a=3.173$ Å. This corresponds to an interlayer spacing $d=2.244$ Å that agrees with the experimental value $d=2.237$ Å.[16] The W(110) surface is modeled by a periodic five-layer slab with a supercell vector along the normal to the surface (Z axis) of $12d$. Under these conditions we relax the interlayer distance to get the equilibrium geometry of the W(110) surface in absence of adsorbates. Keeping the third layer fixed, the first and fifth layers are shifted inwards by 0.084 Å, whereas the second and the fourth layers experience an outwards shift of 0.002 Å. The relaxation of the topmost layer is consistent with recent experimental and theoretical values.[16,17] Next, we proceed to calculate the N/W(110) PES and the N_2/W(110) PES using a (2×2) surface structure and keeping the relaxed geometry of the slab along the Z axis frozen. Therefore, the value of the atomic and molecular coverages is 0.25 and the slabs are separated by 18.16 Å of vacuum. The Brillouin-zone integration is performed with a $4\times4\times1$ Monkhorst-Pack grid of special k points.

B. N/W(110) PES

At large distances from the surface, the N atom hardly interacts with the surface and an adequate description of the ground state (^4S for N in the gas phase) requires a spin polarized calculation. However, we checked that the spin polarized PES converges to the non-spin-polarized PES for $Z\leqslant2.5$ Å. This is precisely the region where the corrugation is relevant. Non-spin-polarized energies are calculated for 13 different sites over the surface unit cell, which, by symmetry, provide information on the 15 sites depicted in Fig. 1(b) by black and white circles.[18] In particular, we use a Z grid of 41 points that goes from 1.6 Å below the surface to 5.2 Å above the surface. In addition, spin polarized calculations are made for various atom sites for $Z>2.5$ Å in order to build the full spin polarized three-dimensional (3D) PES. The zero potential energy is taken as the energy obtained in a spin polarized calculation of the N atom midway between two slabs. The energy has a minimum of −6.86 eV when N is at $Z=1.15$ Å over the fourfold hollow site. The experimental adsorption energy is −6.6 eV.[1,19]

The 3D N/W(110) PES is constructed by interpolating the *ab initio* data with the 3D CRP explained in Ref. 12. Briefly, the 3D potential energy V^{3D} is written as

$$V^{3D}(\mathbf{R}) = I^{3D}(\mathbf{R}) + \sum_{i=1}^{n} V^{1D}(|\mathbf{R}-\mathbf{R_i}|), \quad (1)$$

where V^{1D} is a pair potential describing the interaction between the N and the ith W atoms located at positions $\mathbf{R}\equiv(X,Y,Z)$ and $\mathbf{R_i}\equiv(X_i,Y_i,Z_i)$, respectively. Here, we use the potential calculated for N over a top site, i.e., $V^{1D}(|\mathbf{R}-\mathbf{R_i}|)=V^{3D}(0,0,|\mathbf{R}-\mathbf{R_i}|)$. The sum on the right-hand side of Eq. (1) runs over all slab atoms that give a nonzero contribution to V^{1D}. In practice, we include the 28 atoms from the first and second layers that are separated by a distance $d<5.2$ Å from the irreducible zone [shaded area in Fig. 1(b)]. The resulted interpolation function I^{3D} is a smooth function that can be easily interpolated over X, Y, and Z through a third order 3D spline interpolation. We have checked the accuracy of the constructed 3D PES by comparing a set of *ab initio* values not used in the interpolation with interpolation results. The errors are small (5–15 meV) for $Z\gtrsim1.15$ Å.

C. N_2/W(110) PES

For checking purposes, we first perform a spin polarized calculation of the binding energy and bond length of the N_2 molecule situated midway between two slabs (9.082 Å above the surface) that gives $E_b=9.953$ eV and $r_{eq}=1.1125$ Å. These values can be compared with the experimental values of 9.803 eV and 1.0975 Å,[20] respectively. Since the ground state of N_2 in the gas phase is a singlet state, we perform an unpolarized calculation of the full N_2/W(110) 6D PES. *Ab initio* data are calculated for 30 different configurations that are defined by the molecular orientation (θ,φ) and the position of the molecular center (X,Y) over the surface unit cell. For each configuration, we calculate a two-dimensional (2D) cut of the PES with r varying from 0.7125 to 2.3125 Å in a nonequidistant grid of 11 points and Z from 0.5 to 4.5 Å by steps of 0.25 Å. The potential energies are calculated for the following configurations [black circles in Fig. 1(b)]:

- Five configurations over top site ($X=0$, $Y=0$): $\theta=0°$, $\theta=90°$ with $\varphi=0°$ and $\varphi=54.73°$, and $\theta=45°$ with $\varphi=0°$ and $\varphi=90°$.
- Six configurations over hollow site ($X=a/2$, $Y=0$). We add to the five previous orientations: $\theta=45°$ and $\varphi=54.73°$.
- Six configurations over bridge site ($X=a/4$, $Y=a\sqrt{2}/4$): $\theta=0°$, $\theta=90°$ with $\varphi=0°$, $\varphi=54.73°$, and $\varphi=125.27°$ and $\theta=45°$ with $\varphi=54.73°$ and $\varphi=125.27°$.
- Six configurations over short top-hollow site ($X=a/4$, $Y=0$): $\theta=0°$, $\theta=90°$ with $\varphi=0°$ and $\varphi=54.73°$, and $\theta=45°$ with $\varphi=0°$, $\varphi=90°$, and $\varphi=180°$.
- Seven configurations over long top-hollow site ($X=a/4$, $Y=a\sqrt{2}/4$): $\theta=0°$, $\theta=90°$ with $\varphi=0°$ and $\varphi=54.73°$, and $\theta=45°$ with $\varphi=0°$, $\varphi=54.73°$, $\varphi=90°$, and $\varphi=270°$.

These *ab initio* data are interpolated with the 6D CRP.[12] Now, the full potential energy V^{6D} is written as

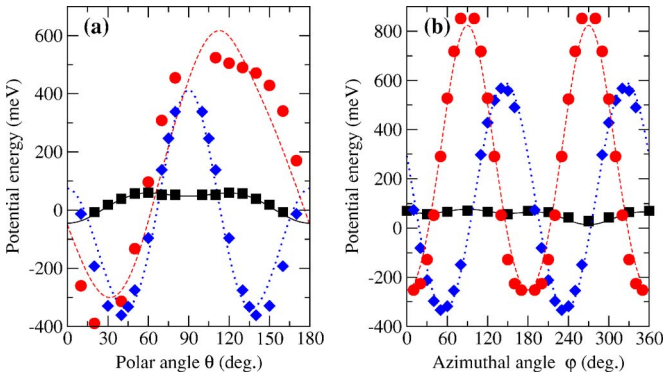

FIG. 2. (Color online) Comparison between interpolated potential energies (lines) and *ab initio* values not used in the interpolation procedure (symbols). (a) Variation with θ for the molecule over top site at $Z=3.5$ Å with $\varphi=0°$ (black full line and squares), long top hollow at $Z=2.5$ Å with $\varphi=270°$ (red dashed line and circles), and bridge at $Z=2.25$ Å with $\varphi=54.73°$ (blue dotted line and diamonds). In all the cases $r=r_{eq}$ (b) Variation with φ for the molecule over long top hollow with $Z=3.5$ Å, $r=r_{eq}$, and $\theta=60°$ (black full line and squares); bridge with $Z=2.25$ Å, $r=r_{eq}$, and $\theta=45°$ (blue dotted line and diamonds); and long top hollow with $Z=1.75$ Å, $r=1.2125$, and $\theta=90°$ (red dashed line and circles).

$$V^{6D}(X,Y,Z,r,\theta,\varphi) = I^{6D}(X,Y,Z,r,\theta,\varphi) + V^{3D}(X_A,Y_A,Z_A) + V^{3D}(X_B,Y_B,Z_B), \quad (2)$$

where V^{3D} is the atom/surface potential energy, $(X_{A,B},Y_{A,B},Z_{A,B})$ are the coordinates of the nuclei, and I^{6D} is the interpolation function. As expected, I^{6D} exhibits a smoother dependence on (X,Y,Z) than V^{6D}. However, it still shows a nonmonotonous dependence on (θ,φ). This forced us to include an unusual number of tilted configurations (12) in order to construct an accurate interpolation. We adopt the procedure of Ref. 12 to interpolate I^{6D} performing, in this case, a third order spline interpolation over the coordinates of the molecular center (X,Y,Z) and over the internuclear distance r. For each site, interpolation over θ and φ is done with a Fourier series expansion.

The accuracy of the constructed 6D PES is checked by comparing the interpolated values with calculated *ab initio* data not included in the interpolation procedure. The main source of errors is caused by the difficulty to interpolate over θ and φ the still corrugated I^{6D}. This problem has been reasonably controlled by our choice of configurations. Figure 2 shows the comparison between interpolated (lines) and *ab initio* (symbols) energies for some of the configurations that will play a crucial role in the dynamics. The region above 3.0 Å is important at low energies. There, the errors are really small ($\leqslant$15 meV). At distances closer to the surface, where corrugation is stronger, the inaccuracy is larger. The interpolation over θ for the long top hollow site is an example of one of the lowest accuracies reached in this region. Errors for those configurations playing a role in the dissociation process are typically less than 100 meV at these distances. Finally, below 1.75 Å the errors can be slightly larger. However, a good accuracy in this region is not so important since dissociation is already decided before reaching these distances.

Figure 3 shows the variation of the potential energy for various configurations of the N_2 molecule approaching the surface with r_{eq}. The zero energy is taken as the energy of the N_2 molecule at its equilibrium position midway between two slabs. All calculated configurations, except the top-vertical one, exhibit a potential barrier at distances relatively far from the surface ($Z\geqslant 3.75$ Å). This is more clearly seen in the right hand plot. The most repulsive configuration that prevents the molecule from getting closer than 4 Å corresponds to the molecule perpendicular to the surface over a hollow

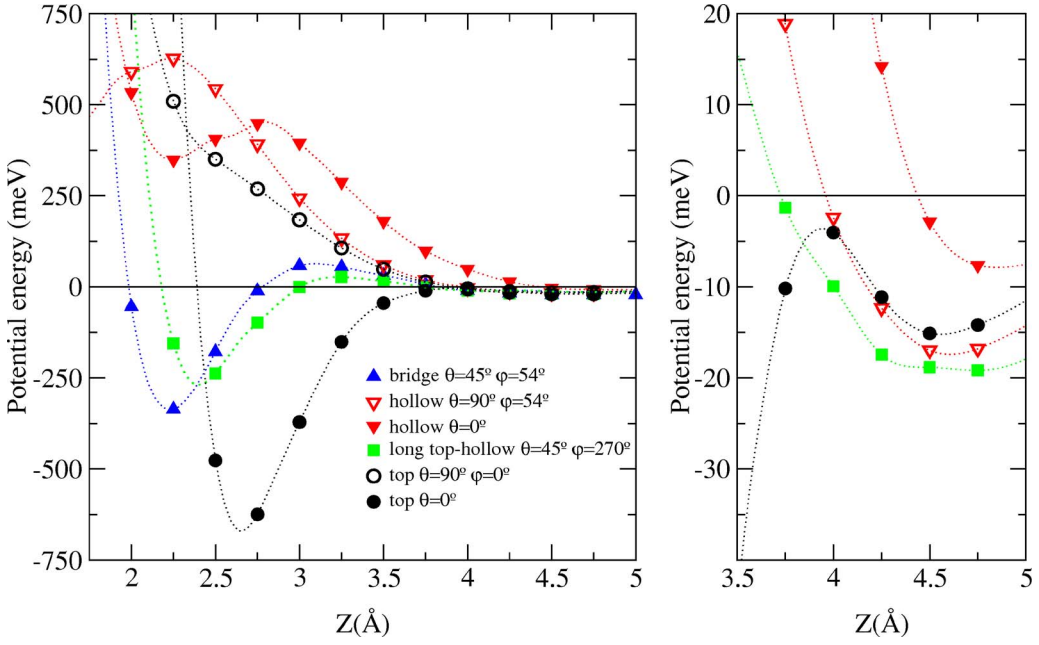

FIG. 3. (Color online) Dependence of the *ab initio* potential energy for N_2/W(110) on the distance of the molecular center from the surface, Z for fixed X, Y, θ, and φ. In all cases, the internuclear distance is also fixed to the equilibrium bond length, $r_{eq}=1.1125$ Å. The *ab initio* data are represented by symbols. Interpolations of the calculated data are shown by dotted lines. The selection includes the most repulsive (hollow $\theta=0°$) and the most attractive (top $\theta=0°$) configurations. The plot on the right shows a zoom of the potential energy at large distances for some of these configurations.

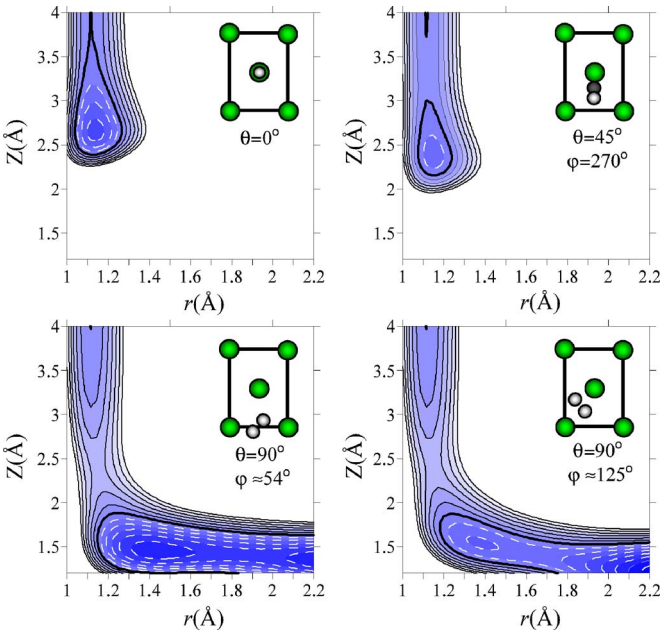

FIG. 4. (Color online) (r,Z) cuts of the N_2/W(110) PES for different configurations of N_2. The molecular orientation and position over the surface unit cell is schematically depicted in each contour plot. The thick solid lines correspond to zero potential energies. Contour lines separate intervals of 0.2 eV. Full (dashed) contour lines correspond to positive (negative) values of potential energy.

site. Also notice that the attraction to the top-vertical well becomes important once the molecule is at $Z=3.5-3.75$ Å. As discussed in the next section, these features determine the N_2 dissociation dynamics at low energies.

Another remarkable feature is the presence of possible molecular adsorption sites. In order to identify them, it is necessary to confirm the existence of molecular configurations with a local minimum in the 6D PES. Following the methodology of Ref. 21, we find a minimum energy of roughly 705 meV that corresponds to the molecule perpendicular over a top site at $Z\approx 2.6$ Å and $r\approx r_{eq}$. We find that the minimum energy measured from the bottom of the well that allows the molecule to escape toward dissociation is ≈395 meV. This potential well can be associated with the γ-N_2 molecular state observed experimentally, although our theoretical adsorption energy is larger than the values of 260 and 450 meV estimated from temperature desorption[22] and electron impact techniques,[23] respectively.

A selection of calculated (r,Z) cuts is shown in Fig. 4. The potential well associated with the top-vertical configuration is quite sharp and narrow. The upper plot on the right shows the calculated configuration at long top hollow that allows the molecule to leave the well and get closer to the surface. The lower 2D cuts correspond to the two calculated configurations that allow dissociation. In both cases, the molecular axis is parallel to the surface and pointing toward hollow sites, the position at which the N atom adsorbs. A simple and "static" analysis of these 2D cuts, in which the molecule is forced to approach the surface with a fixed configuration, leads to the erroneous conclusion that the dissociative reaction in the N_2/W(110) system is activated. Since the molecular initial configuration may be continuously altered along the trajectory due to its interaction with the surface, a conclusion based only on the analysis of the PES for the different but fixed configurations can be misleading.[24–26] We have carefully checked that there are configurations without energy barriers at large distances to the surface, in contrast to the calculations of Ref. 11. Furthermore, we did find nonactivated paths for dissociation, i.e., reaction paths in 6D, which allow to reach dissociation with a potential energy staying always below zero. A detailed description of those nonactivated paths that play a role in the dynamics is given in next section.

III. DISSOCIATIVE DYNAMICS OF N_2 MOLECULES ON THE W(110) SURFACE

The dissociative adsorption energy is defined as the difference between the binding energy of the molecule in gas phase and the energy of two N atoms adsorbed on the surface. In our calculations, the former is 9.953 eV and the latter 13.72 eV. As a result, the dissociative adsorption of N_2 on W(110) is an exothermic reaction that liberates 3.767 eV per molecule. We have analyzed the dynamics of such a reaction by classical trajectory calculations, using a conventional Monte Carlo procedure to sample the initial (X,Y) values over the unit cell and the molecular orientation. Each trajectory starts at $Z=7.5$ Å from the surface. At this distance, the PES for N_2 at its equilibrium bond length r_{eq} is roughly zero. Under these conditions we perform a pure classical (C) calculation, in which the molecule is initially at r_{eq}, and a quasiclassical (QC) calculation that includes the initial zero point energy of the molecule. In the latter, we use a classical microcanonical distribution of r and its conjugate momentum p_r for N_2 in its ground rovibrational state. The initial zero point energy, $E_0=0.1423$ eV, is derived from the variation of the molecular energy with the internuclear distance, $E(r)$. This function is obtained interpolating the *ab initio* energies calculated with the molecule midway between two slabs.

In the trajectory calculations we distinguish the following events: (i) dissociation, when the molecule internuclear distance reaches the value $r=2.3125$ Å (i.e., $\sim 2r_{eq}$) with a positive radial velocity; (ii) reflection, when the molecular center reaches the initial starting distance of 7.5 Å with a positive Z velocity; and (iii) molecular trapping, when the molecule after 15 ps is neither dissociated nor reflected.

The dissociation probability $S_0(E_i)$ with perpendicular incidence $\Theta_i=0°$ and initial kinetic energy E_i is derived from the evaluation of 5000 trajectories. The qualitative behavior of $S_0(E_i)$ obtained from C and QC calculations is similar, although the values are slightly smaller in the former than in the latter. The difference is less than 5% for $E_i>700$ meV and about 15%–25% as the energy decreases to ~50 meV. At very small energies ($E_i<30$ meV), where the sticking coefficient is almost negligible, the difference is of ~80%.

The QC dissociation probability is plotted in Fig. 5 by small black circles. Except for the small energy range of 200–400 meV, the dissociation probability increases with E_i. Furthermore, S_0 is negligible ($\sim 10^{-3}$) for initial kinetic energies below 30 meV, despite there exist nonactivated

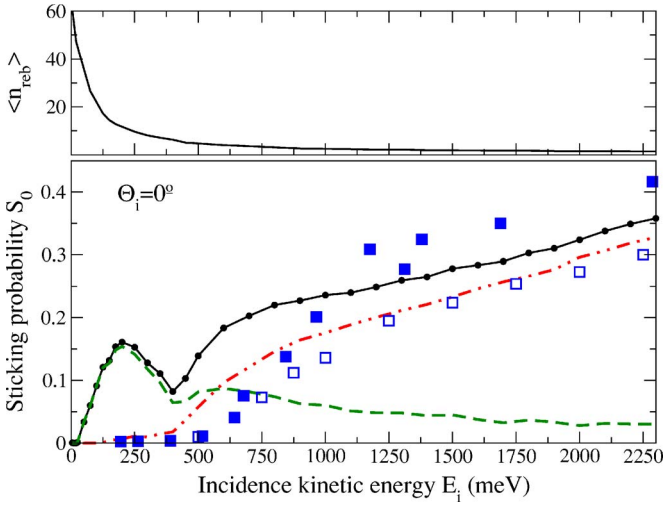

FIG. 5. (Color online) Dissociative sticking probability S_0 as a function of the initial kinetic energy E_i for an incidence angle $\Theta_i=0°$. The small black circles represent our theoretical results obtained from a quasiclassical calculation (see text for details). The red dash dotted and green dashed lines show the contribution to S_0 coming from the direct and the indirect channels, respectively. The blue close squares are the experimental results of Ref. 6 and blue open squares are the experimental results as quoted in Ref. 8. In both cases the surface temperature is $T_s=800$ K. The mean number of rebounds $\langle n_{\mathrm{reb}}\rangle$ for the dissociating molecules is represented as a function of E_i in the upper figure.

paths leading to dissociation. The $N_2/W(110)$ system has been traditionally considered an activated system in view of the *S*-like dependence of the experimental initial sticking coefficient $S_0(E_i)$ (blue squares in Fig. 5). Our results show that an increasing behavior of S_0 with E_i is not necessary an experimental evidence that unambiguously identifies activated systems.

A detailed analysis of our results shows that the trajectories followed by the molecules under normal incidence conditions ($\Theta_i=0°$) are rather complex and imply energy exchange among the different molecular degrees of freedom. A clear feature arising from this energy exchange is the bouncing observed in many trajectories, particularly in those followed by molecules with low and intermediate initial kinetic energies ($E_i\leqslant 400$ meV). The upper plot in Fig. 5 shows how the mean number of rebounds $\langle n_{\mathrm{reb}}\rangle$ experienced by the dissociating molecules rapidly decreases as E_i increases. In order to get a better insight into the mechanism driving the dissociative reaction, we separate $S_0(E_i)$ into two contributions: a direct process in which the molecules dissociate with almost no rebounds (less than four) and an indirect process (named "dynamic trapping" following earlier work[27,28]), in which dissociation takes place after four or more rebounds. Our results show that whereas the latter mechanism is ruling dissociation for energies $E_i\leqslant 400$ eV (green dashed curve in Fig. 5), the former is dominant at higher energies (red dash-dotted curve in Fig. 5).

A statistical analysis of the trajectories with $\Theta_i=0°$ reveals a different behavior of the surface reactivity in three different energy regimes that can be roughly defined by (i) $E_i>400$ meV, (ii) 200 meV$<E_i<400$ meV, and (iii) $E_i<200$ meV. These energy regimes are apparent in the $S_0(E_i)$ curve by sign changes in its derivative.

A. High energies $E_i>400$ meV

The dissociative reaction under normal incidence conditions and high incident energies is a rather direct process determined by the characteristics of the PES at distances close to the surface ($Z\lesssim 2$ Å). For these incident energies, the molecules are able to overcome the potential energy barriers appearing for most of the configurations in the entrance channel (see Fig. 3) and reach the surface without going through the top-vertical well.

A schematic idea of the dynamics leading to dissociation for these energies can be visualized with help of Fig. 6. This figure shows the evolution of the dissociating molecules with initial kinetic energy $E_i=500$ meV. Upper plots represent the position of the molecular center over the surface unit cell [shown in Fig. 1(b)], when the molecule first reaches a given distance from the surface *Z*. The rotational motion of these dissociating molecules is represented in the lower plots that show the corresponding polar distribution as they approach the surface. Notice that the latter is symmetric (within statistical errors) with respect to $\theta=90°$. The reflection process can be followed by comparing the dissociative probability of 14% with the percentage of molecules that reaches *Z* (N_z value given on each column). Close to the surface, N_z can be smaller than the dissociation probability, showing that some molecules have been already dissociated at a higher *Z*.

The initial (X,Y) position and θ distribution of the dissociating molecules are roughly the ones represented at $Z=4.5$ Å. From this distance down to $Z=2$ Å, the molecules experience only a slight motion along the surface and the PES corrugation is mainly reflected through an induced rotational motion. The fact that the molecular center motion remains nearly normal explains why most molecules reaching $Z=2$ Å are those initially over the bridge or long top-hollow sites: the others meet a potential wall and are reflected. Finally, dissociation takes place from $Z\sim 1.3$ Å to $Z\sim 1.1$ Å, with the molecular center located along the region joining hollow-bridge-hollow sites. At this point, most of the molecules are already oriented parallel to the surface and pointing toward hollow sites, the position where N atoms adsorb.

B. Intermediate energies 200 meV$<E_i<$400 meV

The dissociative dynamics at these energies is mostly an indirect process characterized by the dynamic trapping of the molecules in the vicinity of the potential well.

The various steps in the dissociation reaction can be unraveled with the help of Fig. 7. At $Z=4.5$ Å, the molecular (X,Y) position and the polar orientation remain roughly unchanged from their initial values. From $Z=4.5$ Å to $Z=3.0$ Å, the molecules rotate toward tilted configurations of $\theta\sim 60°$, approaching the surface over the same initial (X,Y) position. From $Z=3.0$ Å to $Z=2.5$ Å, the molecules are accelerated toward the well and, consequently, oriented nearly normal to the surface. At $Z=2.5$ Å, the spatial distribution (top panel) is centered over the top site and the angular one around $\theta\sim 30°$. Because of the large PES corrugation in the latter region, energy is transferred from normal motion to other degrees of freedom and the molecule is dynamically

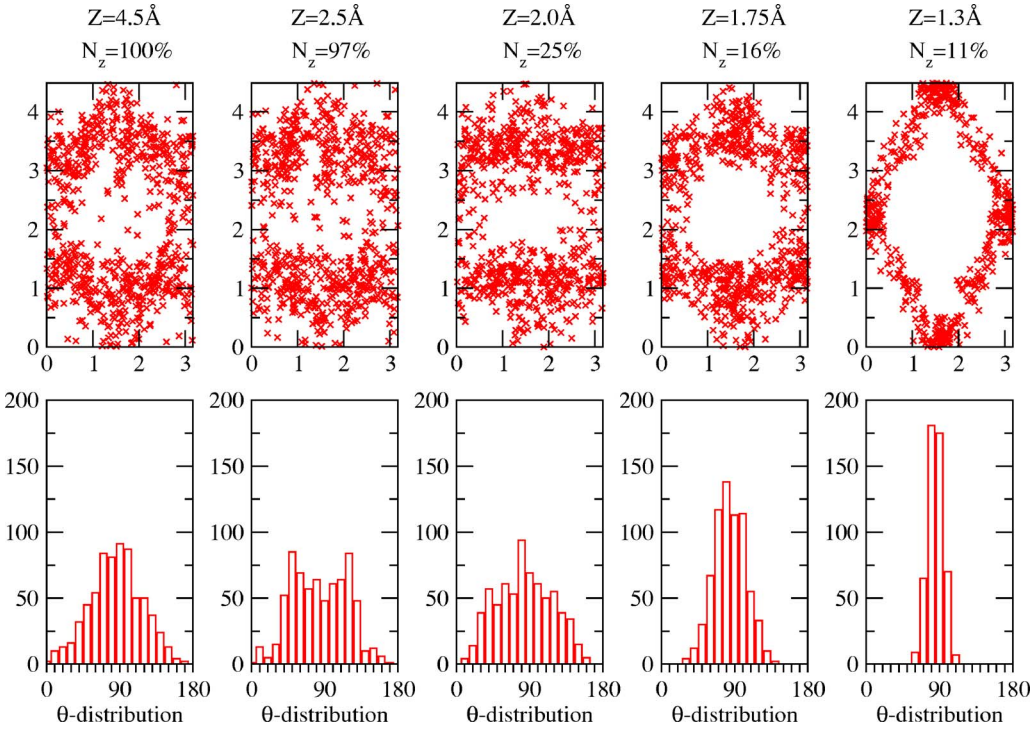

FIG. 6. (Color online) Evolution of the molecules that eventually dissociate. The incidence is normal to the surface and the initial kinetic energy is 500 meV. Upper plots: position of the molecular centers over the surface unit cell when first reaching the distance Z given above each column. The N_z value is the fraction of all incident molecules that reach Z. Lower plots: distribution over polar angles θ for a binning of 10°. The dissociative sticking probability is 14%.

trapped in the well. On average, it stays more than 1 ps in the well before it finds its way toward dissociation. The final dissociating configuration is the same as that for higher energies and is reached when the distance to the surface is ~1.3 Å.

The comparison between Figs. 6 and 7 reveals a complete change in the dynamics between the high and intermediate energy ranges. First, the initial distribution of molecules that eventually dissociate is uniform in the intermediate energy range and much more localized for high energies. Second, for Z=2.5 Å, the distribution is centered on top sites for intermediate energies while hardly any flux

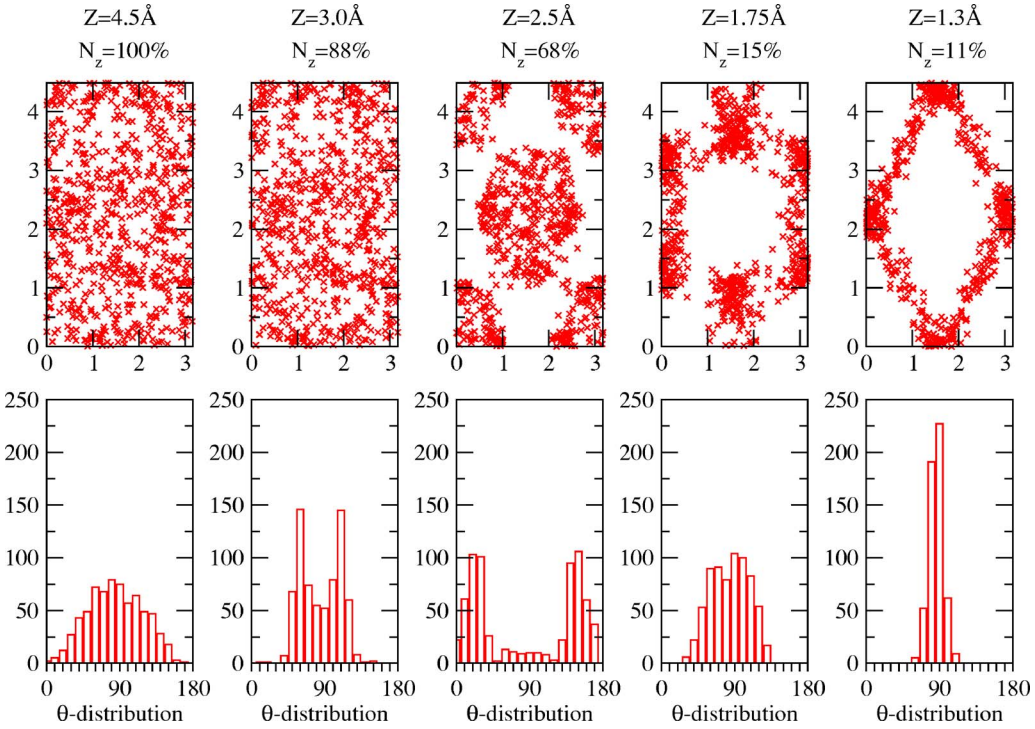

FIG. 7. (Color online) Same as Fig. 6 for E_i=250 meV. The dissociative sticking probability is 15%.

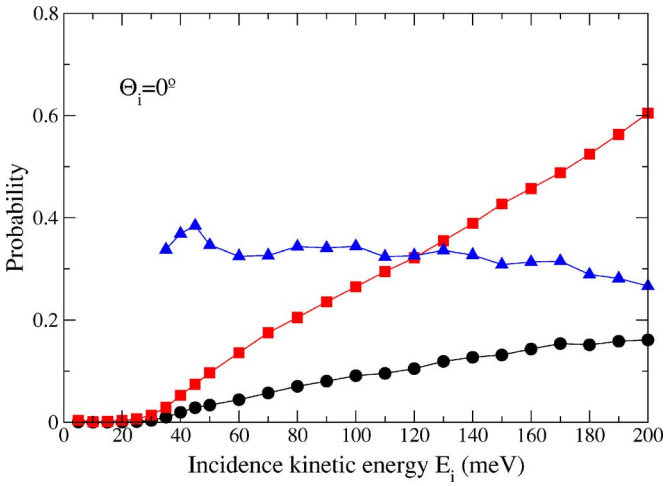

FIG. 8. (Color online) Probability of the N_2 molecules to arrive at $Z=3.0$ Å (red squares) as a function of the incident energy and incidence angle $\Theta_i=0°$. The blue triangles show the dissociating probability for those molecules that reach $Z=3.0$ Å. For $E_i<30$ meV, the number of molecules reaching this distance is not enough to get good statistics. The black circles represent the calculated sticking coefficient S_0.

goes through this position at high energies. Both differences are a clear signature of the role played by the well at intermediate energies.

Dynamic trapping is usually associated with an increase of the dissociation probability as the energy decreases[21,27,29] together with a large number of rebounds. This is what we observe in Fig. 5 between 400 and 200 meV. There is a big difference, however, in comparison to the dissociative trapping of the systems studied in Refs. 21, 27, and 29: the sudden decrease of S_0 to almost zero values below 200 meV in N_2/W(110) that points to a new feature dominating the low energy regime.

C. Low energies $E_i<200$ meV

The sharp decrease of S_0 to negligible values at very low energies is striking from a conventional point of view. The existence of nonactivated paths that allow dissociation and the dynamic trapping on a potential well are features that, in principle, should enhance the dissociative reactivity. Figure 8 shows that the surprisingly small value of the dissociation probability at these energies arises from the low probability to approach the well: for kinetic energies below 100 meV, most of the N_2 molecules incident on W(110) are already reflected above $Z=3.0$ Å. The qualitative dependence of S_0 as a function of E_i is already reproduced by the molecules reaching this distance, which can be considered as a rough estimate of the entrance to the well. The low reactivity of the N_2 molecules on W(110) in the thermal energy range is thus a consequence of the PES properties at large distances from the surface.[30] The dissociation probability after being trapped in the well is almost independent of the initial incident energy of the molecule (see Fig. 8). Among those that are able to access the well, about 30% of them are able to eventually dissociate after spending few picoseconds bouncing in the vicinity of the surface.

Details of the dynamics followed by dissociating N_2 molecules in this energy range are shown in Fig. 9. To reach the well, the approaching N_2 molecules are attracted towards the top position while rotating. The few dissociating molecules are initially over bridge, short and long top hollow with an average orientation $\theta\sim 50°$. In the well, the molecules become dynamically trapped until they continue either to dissociation at the surface or reflected back to the gas phase. For $E_i=50$ meV, molecules are trapped in the well region $\sim$10 ps on average. The exit from the well toward

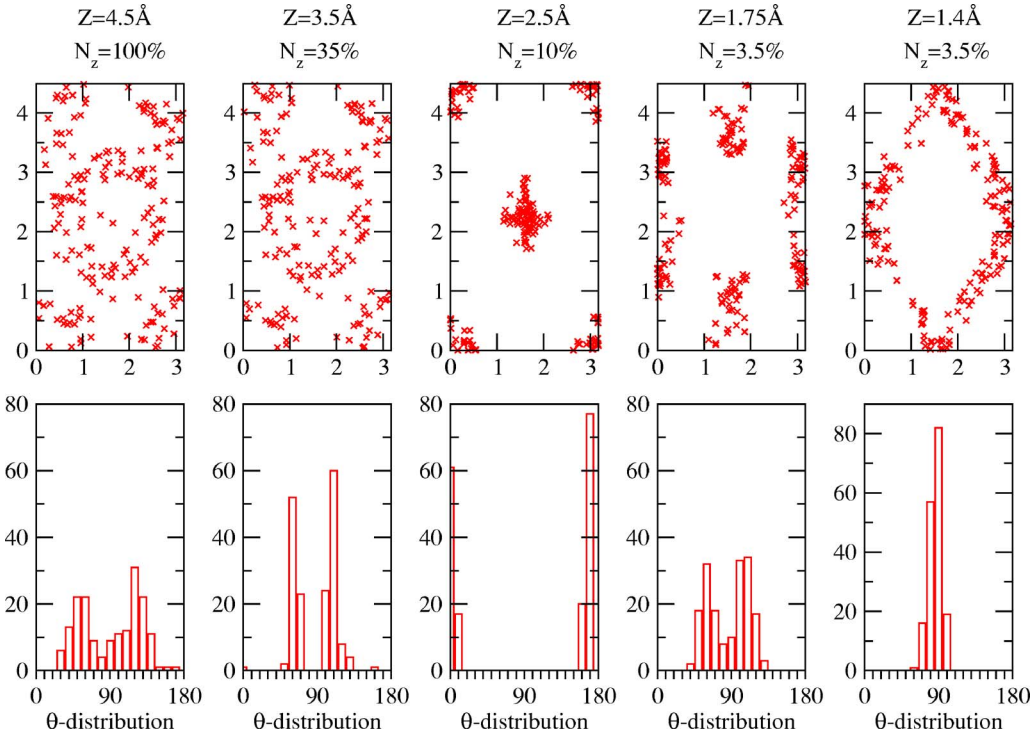

FIG. 9. (Color online) Same as Fig. 6 for $E_i=50$ meV. The dissociative sticking probability is 3.5%.

dissociation takes place at $Z \sim 1.75$ Å with the molecule passing over long top-hollow position in a tilted orientation of $\theta \sim 60°$. Once the molecules arrive to $Z=1.4$ Å, the dissociation path is similar to the ones previously explained.

D. Comparison with experiments

The dissociative chemisorption of N_2 on the W(110) surface has been studied using molecular beam techniques. Figure 5 shows the initial sticking coefficient $S_0(E_i)$ measured at a surface temperature $T_s=800$ K and perpendicular incidence angle.[6,8] It takes values smaller than 3×10^{-3} for $E_i \lesssim 400$ meV, increases rather quickly in the range of 400 meV $< E_i <$ 1200 meV, and levels off at higher E_i. The very small value of $\sim 10^{-3}$ below 400 meV is consistent with thermal desorption measurements performed at $T_s=300$ K.[1,19]

When comparing theory with experiment, it should be kept in mind that our results are for a rigid surface while the measurements were done for a surface temperature of 800 K. Nevertheless, additional test calculations performed with the generalized Langevin oscillator model[31] show a sticking coefficient $S_0(E_i)$ rather similar to the one obtained for the frozen surface. In view of these results, the experiments will be compared with the sticking probability calculated in the frozen model. For $E_i > 1200$ meV, the theoretical results are between the two sets of experimental values (see Fig. 5), reproducing in a quantitative manner the smooth increasing behavior of S_0 up to its maximum value of ≈ 0.35. For 500 meV $< E_i <$ 1200 meV, the theoretical S_0 shows the same qualitative variation with energy as the experiments, while overestimating the reaction probability. The vanishing of S_0 below 30 meV is also reproduced by theory. The main discrepancy appears at energies around 200 meV where a bump, not seen in the experiments, appears in the theoretical S_0. This discrepancy is due to an error in the theoretical description of the indirect channel, as confirmed by the comparison between theory and experiment for an incident angle $\Theta_i=60°$, for which the indirect channel is inhibited. As shown in Fig. 10, S_0 is now dominated by direct dissociation and the agreement with experiment is very good over the whole energy range.

In view of this previous information, it seems that our theoretical results overestimate the dissociative process driven by the indirect channel at energies around 200 meV. There are two possible reasons for that: either the access to the well is inadequately described causing an excess trapping or the balance between dissociation and reflection, once the molecules are trapped, is incorrect. Preliminary dynamics calculations performed with a less accurate 6D PES suggest that the bump appearing at these energies is mainly a consequence of the latter. The less accurate PES was obtained from the interpolation of 1485 *ab initio* energies that only included data for top, hollow, and bridge sites and nontilted configurations. The sticking probability obtained for $\Theta=0°$ is represented in Fig. 11. The bump has almost disappeared and the agreement with experiments achieved at these intermediate energies is paradoxically better. The dynamics for $Z \gtrsim 3.0$ Å (i.e., distances at which molecules are entering to the well) is basically identical to what is obtained with the more accurate 6D PES. Main differences appear at the exit from the well to dissociation ($Z < 2.5$ Å). Hence, the origin of the bump is not in the access to the well but, more likely, in the balance between reflection and dissociation for those molecules that have been trapped.

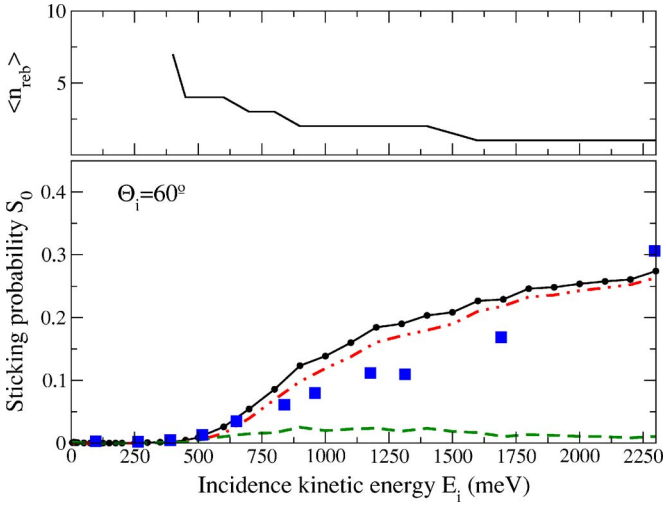

FIG. 10. (Color online) Same as Fig. 5 for $\Theta_i=60°$. The blue squares are the experimental results of Ref. 6 for a surface temperature $T_s=800$ K. The mean number of rebounds is not shown below 400 meV, since the number of dissociating trajectories is not enough to get good statistics.

We have verified that the balance between these two processes is extremely sensitive to details of the PES in the vicinity of the well. More precisely, small differences in the PES in the narrow region that allows the trapped molecules to channel toward dissociation significantly change the dissociation probability for energies around 200 meV and normal incidence, and our results should be taken with caution under these particular conditions. However, the values of the dissociation probability for $E_i < 100$ meV are rather insensitive to the PES characteristics at the well position. In this

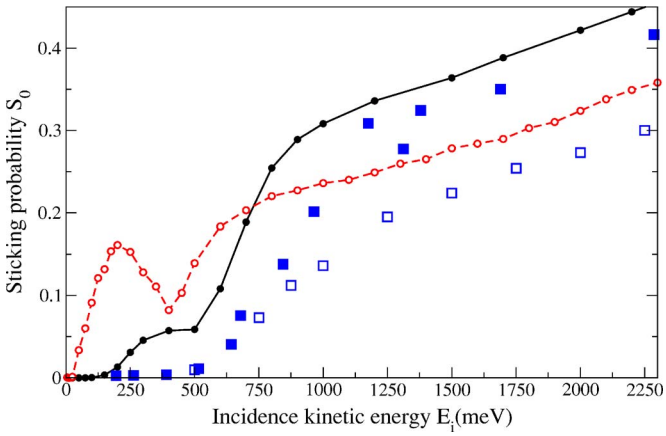

FIG. 11. (Color online) Dissociative sticking probability S_0 as a function of the initial kinetic energy E_i for an incidence angle $\Theta_i=0°$. The black close circles represent our theoretical results obtained from a quasiclassical calculation that uses a less accurate 6D PES (see text for details). The red open circles are results calculated with the more accurate 6D PES. The blue close and open squares are the experimental results of Refs. 6 and 8, respectively, for $T_s=800$ K.

low energy range, the crucial point is the dynamics at distances relatively far from the surface ($Z \sim 3.0$ Å), for which our theoretical results are robust.

IV. CONCLUSIONS

The experimental initial sticking coefficient of N_2 molecules on W(110) takes very small values at low incident kinetic energies and increases rather abruptly with increasing energy above 500 meV. Because of this *S*-like behavior, the present system has usually been considered as an activated system, i.e., the incident molecule would have to overcome a potential barrier. Our theoretical results, based on an *ab initio* PES and classical trajectory calculations, show a similar behavior (except for a spurious bump around 200 meV). In spite of this, we have verified that the system is nonactivated, i.e., that barrierless paths are available and contribute to the dissociation dynamics. This conclusion is striking as it shows that the *S*-like shape cannot be unambiguously allotted to an activated behavior. Below 400 meV, we have shown that a prominent role is played by dynamic trapping about a well that corresponds to the N_2 molecule perpendicular to the surface over a top site. The molecules are effectively attracted by the well and experience an energy transfer from motion normal to the surface toward other degrees of freedom. This causes the dynamic trapping of the molecule in the vicinity of the surface where the molecules start to rebound among the repulsive potential walls. The time spent in this bouncing process before dissociation may vary between 1 and 10 ps depending on the initial kinetic energy of the molecule. We have found that dynamics on the exit channel toward dissociation from the well is, unfortunately, very sensitive to the details of a well localized region of the PES. As a consequence, the theoretical branching ratio between reflection and dissociation is prone to a large uncertainty for trapped trajectories. Notwithstanding, we are still in a position to give an unambiguous explanation to the rapid decrease of the theoretical sticking probability at thermal energies. It arises entirely from the characteristics of the PES at distances larger than 3 Å, in spite of the fact that the latter distance can be reached without having to overcome a potential barrier. At incidence energies above 400 meV, the dissociation process is rather direct: as long as the kinetic energy allows them to overcome the potential slopes, they continue to the surface; otherwise they are reflected.

As far as the comparison with experiment is concerned, the depth of the theoretical well is much larger than the value quoted from temperature desorption and electron impact measurements on N_2 adsorption. However, we find a good agreement when direct sticking dominates, which is the case either for large energies ($E_i > 400$ meV) under normal incidence and for all energies under large incidence angles. The main limitation of our work lies in the use of a rigid surface. This precludes any molecular adsorption, a process which is known to take place for a surface temperature lower than 100 K. However, no significant change with surface temperature is expected for the dissociation probability at thermal and high incidence energies. In the former case, the vanishing of the reaction probability is determined by the dynamics far from the surface where surface temperature is not expected to play a crucial role. In the latter case, dissociation and reflection take place through a direct mechanism which minimizes the interaction time with the surface.

ACKNOWLEDGMENTS

The authors acknowledge partial support by the Basque Departamento de Educación, Universidades e Investigación, the University of the Basque Country UPV/EHU (Grant No. 9/UPV 00206.215-13639/2001), and the Spanish MCyT (Grant No. FIS2004-06490-CO3-00). One of the authors (M.A.) acknowledges financial support by the Gipuzkoako Foru Aldundia. Computational resources were provided by the SGI/IZO-SGIker at the UPV/EHU (supported by the Spanish Ministry of Education and Science and the European Social Fund).

[1] P. W. Tamm and L. D. Smith, Surf. Sci. **26**, 286 (1971).
[2] S. W. Singh-Boparai, M. Bowker, and D. A. King, Surf. Sci. **53**, 55 (1973).
[3] K. Besocke and H. Wagner, Surf. Sci. **87**, 457 (1979).
[4] R. Liu and G. Ehrlich, Surf. Sci. **119**, 207 (1982).
[5] J. C. Lin, N. Shamir, Y. B. Zhao, and R. Gomer, Surf. Sci. **231**, 333 (1990).
[6] H. E. Pfnür, C. T. Rettner, J. Lee, R. J. Madix, and D. J. Auerbach, J. Chem. Phys. **85**, 7452 (1986).
[7] J. Lee, R. J. Madix, J. E. Schlaegel, and D. J. Auerbach, Surf. Sci. **143**, 626 (1984).
[8] C. T. Rettner, E. K. Schweizer, and H. Stein, J. Chem. Phys. **93**, 1442 (1990).
[9] J. W. Gadzuk and S. Holloway, Chem. Phys. Lett. **114**, 314 (1985).
[10] A. Kara and A. DePristo, Surf. Sci. **193**, 437 (1988).
[11] C. Corriol and G. R. Darling, Surf. Sci. **557**, L156 (2004).
[12] H. F. Busnengo, A. Salin, and W. Dong, J. Chem. Phys. **112**, 7641 (2000).
[13] G. Kresse and J. Hafner, Phys. Rev. B **47**, 558 (1993); **48**, 13115 (1993); G. Kresse and J. Furthmüller, Comput. Mater. Sci. **6**, 15 (1996); Phys. Rev. B **54**, 11169 (1996).
[14] D. Vanderbilt, Phys. Rev. B **41**, 7892 (1990).
[15] M. Methfessel and A. T. Paxton, Phys. Rev. B **40**, 3616 (1989).
[16] G. Teeter, J. L. Erskine, F. Shi, and M. A. Van Hove, Phys. Rev. B **60**, 1975 (1999).
[17] M. Arnold, G. Hupfauer, P. Bayer, L. Hammer, K. Heinz, B. Kohler, and M. Scheffler, Surf. Sci. **382**, 288 (1997).
[18] The sites in the irreducible unit cell that can be related by symmetry considerations are (i) the two top sites and (ii) the two sites midway between top and bridge positions.
[19] C. Somerton and D. A. King, Surf. Sci. **89**, 391 (1979).
[20] *CRC Handbook of Chemistry and Physics: A Ready-Reference Book of Chemical and Physical Data*, edited by R. C. Weast (CRC, Boca Raton, FL, 1986).
[21] G. Volpilhac and A. Salin, Surf. Sci. **556**, 129 (2004).
[22] J. T. Yates, Jr., R. Klein, and T. E. Madey, Surf. Sci. **58**, 469 (1976).
[23] Q.-J. Zhang, J. C. Lin, N. Shamir, and R. Gomer, Surf. Sci. **231**, 344 (1990).
[24] A. Gross and M. Scheffler, Phys. Rev. B **57**, 2493 (1998).
[25] H. F. Busnengo, W. Dong, and A. Salin, Chem. Phys. Lett. **320**, 318 (2000).
[26] C. Díaz, J. K. Vincent, G. P. Krishnamohan, R. A. Olsen, G. J. Kroes, K. Honkala, and J. K. Nørskov, Phys. Rev. Lett. **96**, 096102 (2006).
[27] C. Crespos, H. F. Busnengo, W. Dong, and A. Salin, J. Chem. Phys. **114**, 10954 (2001).
[28] H. F. Busnengo, C. Crespos, W. Dong, A. Salin, and J. C. Rayoz, Phys. Rev. B **63**, 041402 (2001).
[29] M. A. Di Césare, H. F. Busnengo, W. Dong, and A. Salin, J. Chem. Phys. **118**, 11226 (2003).
[30] M. Alducin, R. Díez Muiño, H. F. Busnengo, and A. Salin, Phys. Rev. Lett. **97**, 056102 (2006).
[31] H. F. Busnengo, M. A. Di Césare, W. Dong, and A. Salin, Phys. Rev. B **72**, 125411 (2005).